Chapter 5

HyDRa: Vortex Polishing with a Deterministic Hydrodynamic Radial Polishing Tool

Erika Sohn, Esteban Luna, Elfego Ruiz, Luis Salas and Joel Herrera

Additional information is available at the end of the chapter

http://dx.doi.org/10.5772/intechopen.75524

Abstract

This work presents the deterministic hydrodynamic polishing system (HyDRa (HyDRa-dynamic Radial Polishing Tool) based on a polishing tool developed at the Instituto de Astronomía, UNAM. HyDRa is one of several modern deterministic polishing techniques that allow for computer controlled finishing of complex optical surfaces. The HyDRa system is based on a hydrodynamic polishing tool that generates a variable-density abrasive flow that makes possible the production of high-quality optical surfaces of diverse materials. The tool comprises several stacked operational stages that generate a grazwing abrasive flow with a predictable, zero-force erosion footprint on the workpiece that removes material. A recent innovation to the hydrodynamic polishing tool adds a switching capacity to the tool that allows the polishing action to be interrupted at will, without losing the stability of the operating parameters. This further increases the versatility and performance of the tool, since it is now possible to polish only the areas where the surface needs correction. Pulsed polishing also adds several techniques to this polishing method that further increase the system's versatility.

Keywords: deterministic polishing, fluid jet polishing, vortex polishing, pulsed polishing, simultaneous polishing with multiple tools

1. Introduction

As the demand to fabricate larger and increasingly complex aspheric optics becomes more common, the need for deterministic polishing tools which can meet these demands has motivated the development of the hydrodynamic, polishing tool (HyDRa).

The HyDRa polishing tool [1, 2] is a non-contact, zero-force hydrodynamic tool that rotationally accelerates a slurry and air mixture and expels it tangentially onto the workpiece. It consists of several operational stages: an abrasive suspension (water and polishing grit) is fed to the tool's first operational stage, where it is mixed with air at a controlled pressure in order to produce a variable-density abrasive foam. This foam then enters the rotational acceleration chamber, where it is sped up to high revolutions per minute (RPM). The rotational energy of the flow then turns into radial velocity in a nozzle that forms between the tool's divergent output and the workpiece. In this way, the abrasive particles graze the workpiece in closely tangential trajectories. Thus, the polishing particles generate a shearing action that removes material in a ductile removal process, as described in [3]. The drag generated by this radial flow forms a central low-pressure zone (vacuum) surrounded by a high-pressure ring. As a result, the tool floats over the workpiece, exerting no net force onto it [4], since these regions cancel each other out. This poses many advantages in modern deterministic polishing, in particular the capability of polishing ultra-thin surfaces, such as semiconductor wafers and optical membranes.

The HyDRa tool belongs to the fluid jet polishing (FJP) family, originally developed by Fähnle et al. [5]. Although HyDRa also expels an abrasive suspension onto the surface to be polished, there are several basic operational principles that differ from the classic FJP technique. The FJP method, and most other polishing techniques, needs to apply pressure onto the workpiece, in order to remove material. In some cases, as in the classic FJP technique, the force that is exerted onto the material can be minimized by using a small contact area; see for example [6], where the force on the workpiece is less than 1 N. This however, could represent a trade-off between footprint size and removal rate; removal rates of <0.01 mm^3/h are common for 1–2 μm Cerium oxide polisher [6]. Other deterministic methods, such as ion beam figuring (IBF), are non-contact, zero-force processes that present removal rates of up to 50 mm^3/min [7] without degrading the initial micro-roughness.

2. Polishing with HyDRa

This section describes the generalities of polishing with the HyDRa system. A typical static removal footprint is shown in **Figure 1**.

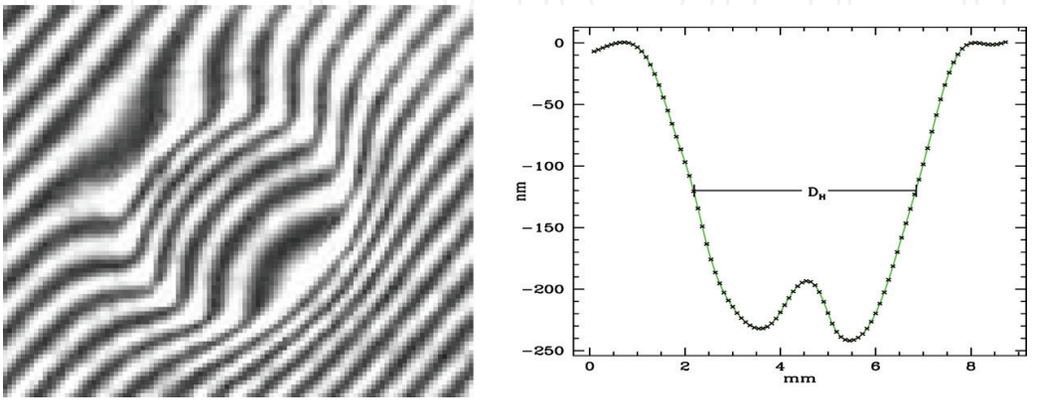

Figure 1. Tool influence function. The image to the right shows the removal function profile extracted from the interferogram to the left. This profile was obtained by operating the tool for 2 s on a fixed position over the workpiece. D_H is the full width at half maximum (FWHM) of the removal function. Tool footprint diameters typically range between 3 and 10 mm, depending on the particular tool.

http://dx.doi.org/10.5772/intechopen.75524

As can be seen, the removal takes place in a ~5 mm diameter region that has an M-shaped geometry. Removal in the central region is about 20% lower than the peripheral region. Removal is a function of slurry density (ρ) and accelerating air pressure (P_T), slurry flow, i.e., flow rate (F_1), and is a linear function of dwell-time. In order to attain deterministic polishing, all tool parameters are controlled with high precision, as described in Section 4.

2.1. The HyDRa polishing rig

The HyDRa tool is part of a complex polishing robot, consisting of a CNC positioning device; a fluid and compressed air control system; a slurry management unit, which stirs the slurry and controls its density; and a software package that obtains error maps from a series of interferometers, and generates dwell-time/constant-velocity PWM trajectories. These trajectories correct the workpiece figure, depending on the selected method (pulsed or continuous operation), as the block-diagram of **Figure 2** illustrates.

The HyDRa tool is attached to a five degree of freedom (DOF) polishing machine with force feedback, based on a 2.4 × 2.4 m Cartesian CNC, with two additional DOF (tip and tilt), implemented by means of a 3-actuator hexapod. This configuration allows the generation and polishing of any surface geometry. Since feedback control keeps all polishing parameters constant, removal is exclusively a function of dwell-time. In this way, figure correction depends on the trajectory followed by the tool and the velocity at each point along it, which requires that the CNC be capable of following five-dimensional, controlled-velocity trajectories. Simultaneously, z-axis movement is controlled so that the tool can accurately follow the surface contour with zero-force. Although the machine's repeatability is around 10 μm, the removal is accomplished with nanometric accuracy due to a load cell that regulates tool height over the workpiece, as reported in [4]. The slurry conditioning unit (SCU) supplies a

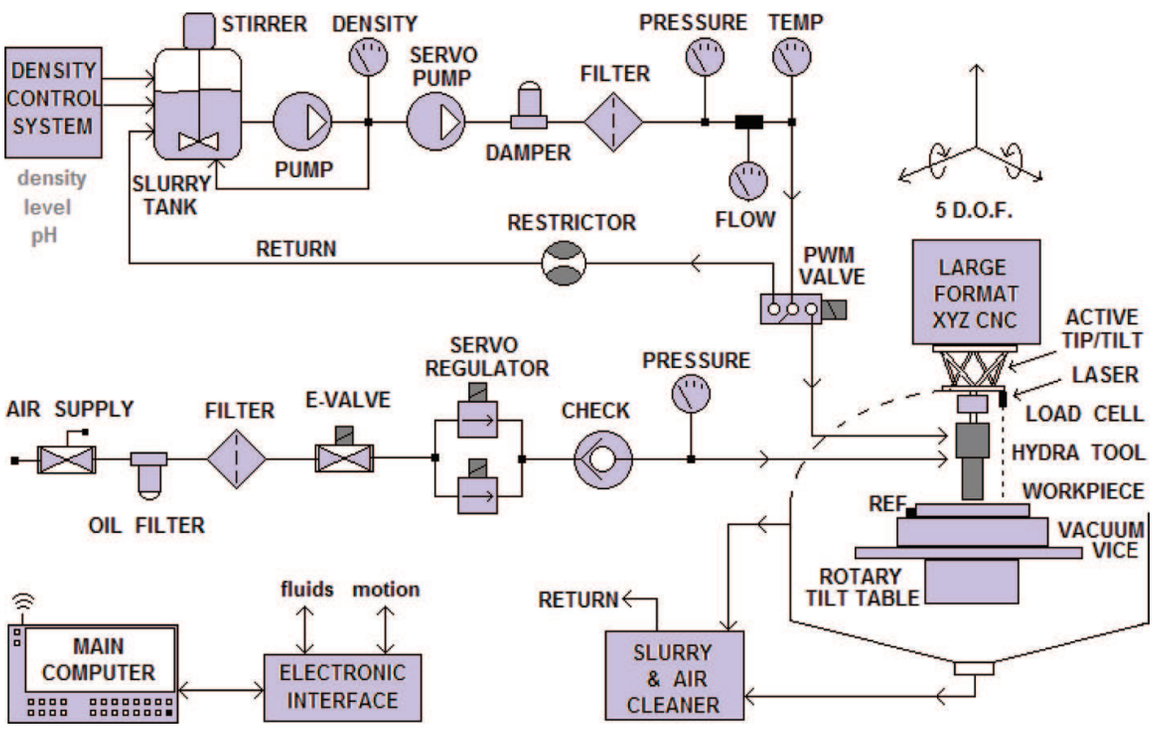

Figure 2. HyDRa polishing process setup, (see text).

density controlled polishing suspension to the HyDRa slurry supply system. It also captures and reincorporates the liquid and atomized slurry that is expelled from the tool. The density is continuously monitored by means of a photodensitometer and controlled by means of polishing-paste and water supply systems. The expelled slurry is captured by the return system, which consists of a blower that reincorporates this slurry and air into the SCU container, forcing the mixture through a washed-air system.

A pump is continually recirculating the polisher in the container, and a derivation supplies filtered slurry to the HyDRa slurry control system. The slurry that flows into the tool is fed by means of a damped-diaphragm DC pump that is feedback-controlled by means of either a flow meter or a pressure sensor. In order to reduce air contamination, the HyDRa system polishes in shallow immersion so that an air-lock for the return system is formed. The HyDRa tool accelerates an abrasive foam, composed of a variable-density suspension of slurry and air created by means of an air control system that regulates the foaming and propelling air pressures using electromechanic air regulators, pressure sensors and control electronics. All polishing parameters are acquired with a data acquisition card, and controlled and visualized in LabView®. The surface is fixed onto the CNC platform as the tool is swept over the surface in a pattern chosen by the user. Pulsed operation of the tool sweeps the tool(s) along the workpiece at a constant velocity, switching the polishing action on and off depending on how much material needs to be removed. The slurry is fed to the tool at controlled pressures and flow rates. The tool is supplied with compressed air to operate the foaming and acceleration stages. The abrasive foam is radially expelled through the tool nozzle onto the surface to be polished, as described above. Tool height is controlled by the feedback variable provided by the load cell, so that the CNC can adjust tool height in order to polish with zero force, as is discussed below.

2.2. Zero-force polishing

One of the central advantages of the HyDRa tool resides in that it can be adjusted to exert zero force on the work surface, while maintaining considerable removal rates (~10 mm^3/h). The flotation effect is described in more depth in this section.

As the HyDRa tool expels the slurry through its nozzle, the rotational energy of the flow is converted to radial velocity. The drag generated by this radial flow produces a central low-pressure zone that is surrounded by a vortex which is in turn confined by a ring shaped, positive thrust zone. This effect differs from the linear jet polishing technique [3, 8] in that, in normal-incidence, classic jets, the pressure profile is represented by a Gaussian distribution, where the maximum is located at the jet's center. In contrast, the pressure distribution of HyDRa on the workpiece presents negative values at the footprint's center and is circumscribed by an annular, positive-pressure region. With this, the force on the workpiece can be adjusted to net zero-force. In **Figure 3a**, footprint pressure vs. distance from the center of the tool is plotted. This was obtained by means of a 0.46 mm diameter orifice connected to a pressure sensor over which the tool footprint was radially scanned. As can be seen, a low pressure zone forms at the central part of the footprint and, as the radius increases, the gauge pressure increases to a maximum. It then falls again as the orifice approaches the tool's outer radius.

http://dx.doi.org/10.5772/intechopen.75524

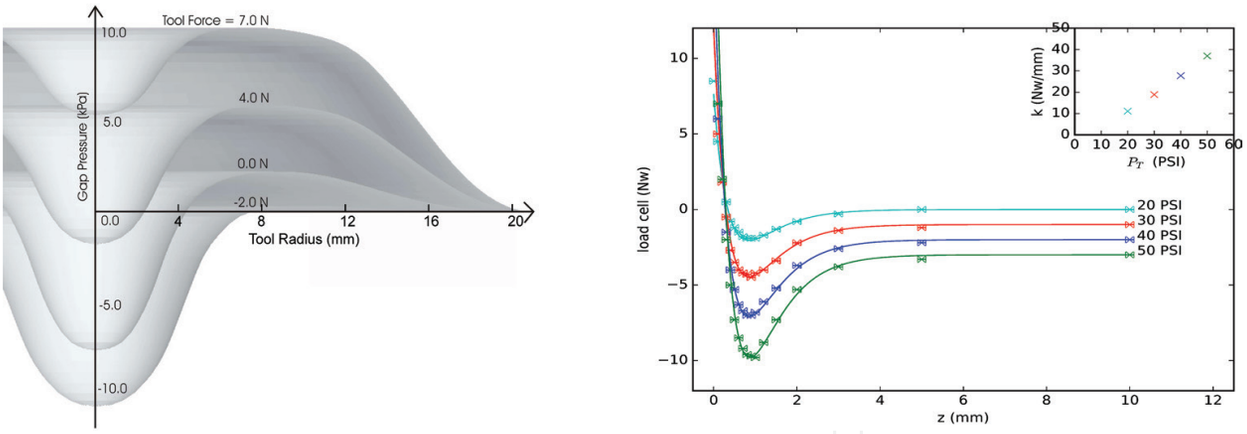

Figure 3. (a) (left) Pressure distribution as a function of tool radius for different operating pressures. (b) (right) Force applied by the HyDRa tool as a function of distance Z from the work surface for accelerating pressures P_T = 20, 30, 40 and 50 PSI. For clarity, a constant offset has been added to the 30, 40 and 50 cases. Typical error bars are 0.1 N for the load cell and 20 μm for the Z position. The solid lines are an analytical function fit derived from a Morse potential. In the upper right inset, the restitution spring constant is shown to be related to P_T. When an external holding force F_h is applied to the tool and pushes it against the workpiece, the vacuum force F_v has a tendency to decrease as the thrust force F_e is increased.

As the tool moves away from the workpiece, the vacuum has a tendency to increase, as the thrust force tends to decrease; in consequence, the balance of these two forces is a function of the tool's distance from the surface to be polished. With this, several operational modes can be achieved, one of them allowing the tool to freely float over the surface without the need to rigidly attach it to a positioning device. In this case, the tool's weight is counterbalanced by the thrust and vacuum forces. When the HyDRa tool is mounted onto a passive hexapod through a load cell, the support force F_h counterbalances the tool weight mg and the remaining forces to zero, while maintaining the tool in a static position.

The load cell value F_h is then used as feedback for the control system to maintain zero force on the workpiece. This is done by adjusting the z-axis of the CNC/hexapod.

We measured the tool and workpiece force interactions as a function of separation. In **Figure 3b**, the overall behavior of this interaction is shown in experiments where slurry accelerating pressures of 20 to 50 PSI and a polishing slurry flow of 5 ml/s were used. The distance over the workpiece was modified from several millimeters, down to a few hundred microns. The values of the load cell F_h were used to obtain the substrate force F_x, as explained above.

When the tool exceeds a certain distance, the workpiece experiences no force (see **Figure 3**). As the tool approaches the substrate, a negative force (attraction) is produced by a vacuum that develops between the workpiece and the HyDRa tool. As the tool further approaches the workpiece, a positive repulsion force is experienced, caused by the thrust force. At a few hundred μm from the workpiece, the vacuum and thrust forces balance each other out to zero. Here the surface can be polished without being deformed by the tool.

The combination of attractive and repulsive forces commonly arises in physical problems. One of such is given by the empirical Morse potential of diatomic molecules $U(z) = B\left(1 - e^{(-\alpha(z-z_m))}\right)^2 - B$, where B is the dissociation potential and z_m is the separation at which the minimum of the potential is

P_T (PSI)	B (N mm)	α (1/mm)	z_m (mm)	k (N/mm)
50	10	1.36	0.36	40
40	7.5	1.36	0.34	27.7
30	5.1	1.36	0.34	18.9
20	3	1.36	0.34	11.1

Table 1. Fitting curve parameters.

reached, which constitutes a stable equilibrium separation. A force can be readily obtained from this potential by calculating its gradient: $F(z) = -\frac{d}{dz}U(z)$. We have plotted this force along the data of the figure by least-squares fitting the three parameters, B, α and z_m; their resulting values are listed in **Table 1**. A reasonable fit is obtained, and some insights may be derived from this exercise. It can be noted that, as the accelerating pressure P_T increases, so does the depth of the potential well and thus the amplitude of the forces involved, as given by the parameter B. However, the minimum of the potential is found roughly at a constant separation z_m of around 340 μm. At this distance, the force derived from the potential is zero (since the derivative of the potential is zero) and the tool floats over the work surface in stable equilibrium. If we approximate the minimum of the potential by a square law (Hooke's law) a restitution spring constant $k = 2\alpha B$ can be obtained, which measures the force with which the stable position is restituted. The values of k are also given in **Table 1**. As indicated in the inset in **Figure 3b**, k is a linear function of the accelerating pressure P_T.

2.3. Tool influence function and removal rates

Several tools have been developed to accommodate for different removal rates that range from 1 to 600 mm^3/h. This section presents measurements of static and volumetric removal rates for a medium removal-rate tool with a nozzle diameter of 3.8 mm. Several polisher grits have been tested: Cerium oxide (Opaline) with a particle size of 1 μm, and aluminum oxide (μ-grit) with particle sizes of 5 and 12 μm, suspended in water at a constant relative density of 1.09. Samples of different materials were polished: standard window glass, water-free fused silica (Infrasil®-302), BK-7 borosilicate, and Ohara's CLEARCERAM-Z® vitroceramic.

The measurements were performed by scan-sliding the tool over the sample at a constant speed and a corresponding zero-force tool height. The resulting cavity was measured interferometrically, and both the volume of removed material and the depth of the cavity were calculated. With these measurements the static removal rate D_S (depth/time) and the volumetric removal rate D_V were then calculated. We performed these measurements at different operational conditions of accelerating pressure (P_T) and slurry flow (f_p). In all cases, the relative density of the slurry was kept at 1.09. In **Figure 4**, the test results are shown. In all three panels, the left vertical axis D_V is related to D_S as $D_V = D_S * A$, where A is the tool footprint area. Each plot indicates the dependence of removal on the accelerating pressure P_T. The top left panel, where Cerium oxide was used, slurry flow f_p values of 3, 5 and 7 ml/s on window glass were tested. These are indicated as numbers on the curve.

http://dx.doi.org/10.5772/intechopen.75524

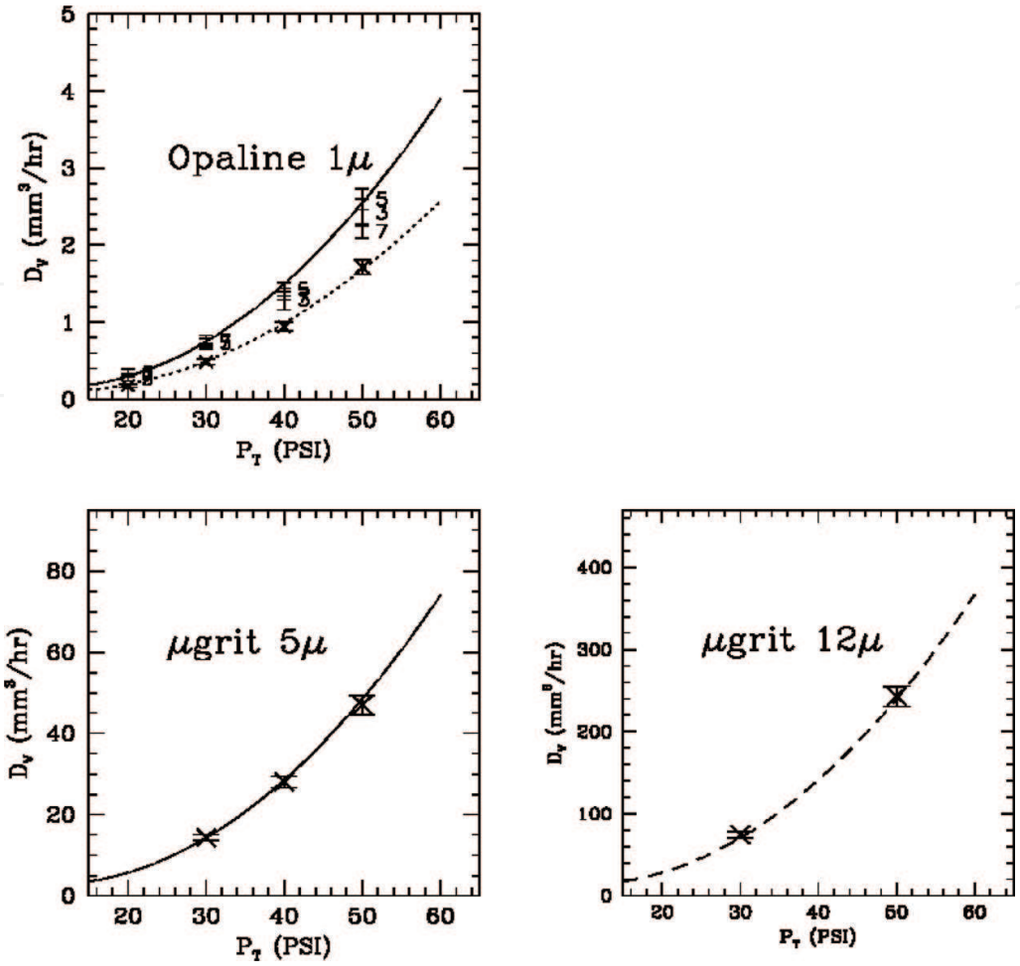

Figure 4. Volumetric removal rate D_V as a function of accelerating pressure (P_T) for various polisher types: 1 μm cerium oxide (Opaline), 5 μm aluminum oxide (μgrit) and 12 μm aluminum oxide. Opaline removal rates are presented for window glass (solid line), fused silica, and borosilicate (dotted line). Removal of μ-grit is shown for window glass and CLEARCERAM®-Z vitroceramic. All fitted curves are versions of the same second order polynomial law, scaled by a factor that is a function of substrate material and particle size (see text). Zero-force polishing was achieved at the corresponding tool height for this effect.

As can be noted, the highest removal rate for this tool is achieved with a slurry flow of 5 ml/s, thus this flow was employed for all consecutive experiments. Removal rates up to 2.5 mm^3/h at 50 PSI are obtained for this polisher. The $f_p = 5$ points are well fitted by a second order polynomial. In the first panel we also show the results of polishing a fused silica sample (crosses). In this case the hardness of the material causes the removal rate to decrease to 66% compared to window glass. The dotted line that fits these values is obtained by multiplying the same D_S polynomial by a small factor. In the lower left panel we tested the removal rate of 5 μm aluminum oxide grit on glass (crosses). The volumetric removal rate rises to ~50 mm^3/h at an accelerating pressure of 50 PSI. The solid line is the D_S polynomial obtained previously, multiplied by 19. Again, a very good fit can be seen. Lastly, in the lower-right panel, the removal rate of aluminum oxide grit (12 μm particle size) on Ohara CLEARCERAM® vitroceramic is shown. Removal was so large that it was impossible to measure it reliably with an interferometer, so the resulting cavity was measured by means of a needle profilometer. Only two points were

taken in this experiment (crosses in the last graph). If the same polynomial D_S were to be fitted (dashed line), it would have to be multiplied by 94. For all cases, the removed volume per abrasive particle is 3 to 5 orders of magnitude lower than the particle's volume. The kinetic energy as well as the grazing incidence associated with both the cerium and alumina particles, creates stresses that are not large enough to produce permanent dents. Resulting typical micro-roughnesses of 2, 24, and 31 nm, for grit sizes of 1, 5, and 12 μm, respectively, are around three orders of magnitude smaller than the particle sizes. These tests demonstrate that independently of grit size and material, as well as substrate hardness, behavior of removal as a function of accelerating tool pressure is comparable, which indicates that the same material removal process discussed above is taking place. The scaling parameter is an indicator of how efficiently a particular abrasive removes material from a surface of a given hardness. All HyDRa tools present this same relationship of removal as a function of P_T and grit size for pressures of up to 90 PSI. Currently, typical removal rates of ~15 mm^3/h @ 90 PSI, using 1 μm Opaline on borosilicate glass, are common.

2.4. Software

The HyDRa trajectory planning tool (HyTPT) is a software package developed specifically for the HyDRa tool [9]. It feeds machining code to a CNC or any computer-controlled positioning device, based on the error map that has been obtained interferometrically. When only one HyDRa tool is available, the amount of material that is removed at each specific position is proportional to the dwell time. This dwell time can be controlled either by the speed of the tool along a given trajectory when the tool is operated in continuous mode, or by the width of the pulses when operated in pulsed mode.

In HyTPT (**Figure 5**) a main window presents the project name and grants the user the ability to go from error maps to machine coordinates in four steps:

1. **Error Map alignment:** This allows the easy alignment of the error map, and the determination of its center, orientation and pixel size. The basic shapes are rectangular, circular, and annular surfaces.
2. **Base trajector:** It is possible to select the base trajectory from a series of curves: from simple raster patterns to more complex curves, such as trochoids and rotating triangles. It is possible to define and analyze each curve from the point of view of trajectory density, total polishing time, and speed at each point, among several others.
3. **Surface shape:** The shape of the surface, currently any on- or off-axis conic section, is defined in this window. The 2-D base trajectory is projected onto this 3-D surface. In addition to the 3-D trajectory the normal vector to the surface at each position is calculated, so that the CNC may orient the HyDRa tool normal to the surface along the trajectory.
4. **Machine coordinates:** A set of alignment tools facilitates the transformation of surface coordinates to machine coordinates. These routines communicate with the CNC machine and are developed for each particular CNC or robot arm to which the HyDRa tool is attached.

http://dx.doi.org/10.5772/intechopen.75524

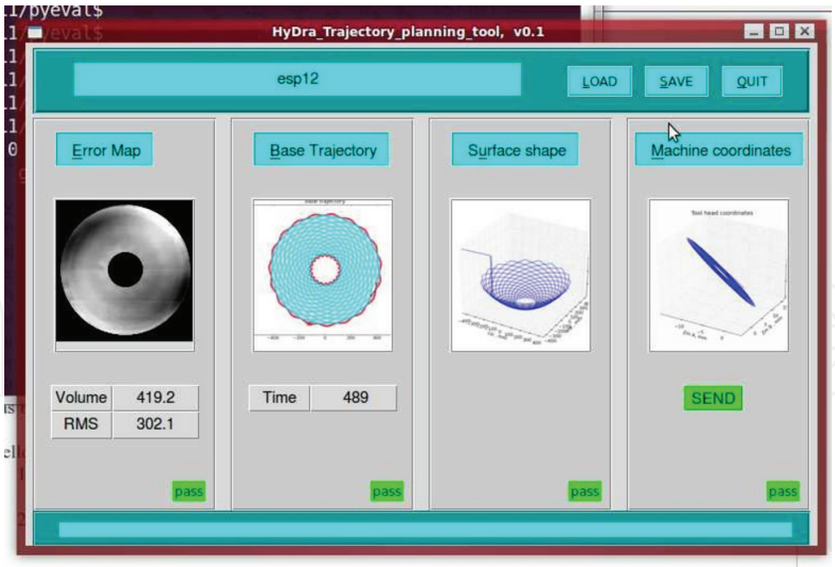

Figure 5. HyTPT software main interface showing all four steps.

Finally, the centering and orientation parameters, nine in total, are determined in order to properly align the system. Once each of these parameters has been calculated, the trajectory is delivered to the CNC machine, or robot arm so it can be executed there.

3. Pulsed polishing

Due to its hydrodynamic properties, the original HyDRa tool [1] does not allow the modification or switching of any of its operational parameters during operation. Therefore, in order to control the removal, dwell time is modified by means of tool velocity. However, there is a maximum tool velocity imposed by CNC limitations, that fixes a minimum, non-zero amount of material that can be removed with the tool. This poses problems for several operational applications, such as zonal corrections, multi-head or tessellated polishing, and edge problems. A new HyDRa tool design (patent pending) [2] overcomes these problems, by switching one of the operational parameters (polisher flow). This enables the pulsing of the abrasive action at will, without affecting tool bias. The ability to operate the HyDRa tool in a switched manner widens its overall performance and efficiency, adding new applications. It is not simple to switch most of the tool's operational parameters during use, since this causes a loss of tool bias, which affects the flotation capability. Restoring these parameters on the fly takes time and produces unwanted effects such as cavitation. This has limited the polishing strategy to making full sweeps of the entire surface. When needing to polish only a small section, the region must be approached with the tool biased, leaving behind an unwanted track and approach and exit marks. A new HyDRa tool design has been developed which allows switching slurry flow without losing tool bias. Switching frequencies of up to 10 Hz, and pulses as narrow as 10 ms, can be achieved with this new tool. This is accomplished by means

of an overdriven electro-valve which is installed in, or close to, the tool. This allows the use of polishing pulses that can be applied on a per-pixel basis or in a continuous scan using pulse width modulation (PWM) techniques. With this feature, dwell time can be controlled below the minimum attainable by a continuous action at the maximum CNC speed.

3.1. Linearity

A pulsed HyDRa tool with a 7 mm footprint has been developed and tested for linearity. **Figure 6a** shows the results of erosion vs. dwell-time. Pulse width was varied at constant increments, starting from 10 ms to a maximum of 500 ms, as the tool was moved at 0.2 mm increments, overlapping 35 times at each tool footprint diameter. The erosion was measured using a Fizeau interferometer and the result was normalized, so that removal corresponded to a single pass of the tool over each point along the line that was polished. Error bars are primarily due to errors produced by the subtraction of the base reference during interferogram reduction. A removal resolution of 0.1 nm/ms can be seen from the data. Noticeable polishing effects were observed at 25 ms. We attribute this effect to the electro-valve response time, which can be improved by using faster actuators.

3.2. Pulsing the polishing process

3.2.1. Pulse width modulation polishing (PWM)

It is now possible to control the duration of a pulse as a fraction of the time it takes the tool to travel a distance of one footprint diameter.

The depth of removed material for a raster scan pattern h, can be given by:

$$h = D_V Y / VS$$

where D_V is the volumetric removal rate, Y is the PWM duty cycle (ON time divided by the period T), V is the CNC velocity, and S is the raster step size. The period of the switching

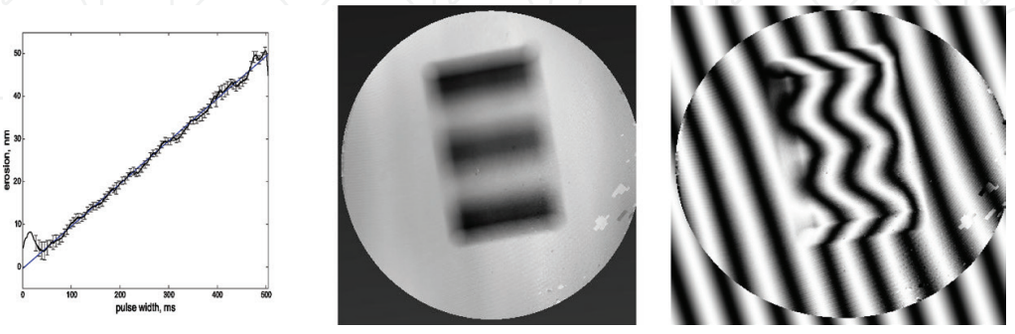

Figure 6. (a) Erosion vs. pulse-width in a linearity test. (b) Response function of the tool for pulsed operation at constant tool velocity. The tool was switched in a PWM mode, with a 50% duty cycle and 100 ms on/off switching times. The raster pattern used to generate this surface is perpendicular to the surface produced in the figure. Pixel size is limited by footprint size. Tool velocity was chosen so the pulses could be resolved independently.

signal is $T = D/V$, where D is the tool footprint diameter. In the time it takes to cross a tool footprint, there is a single pulse whose width can be varied from zero to the entire footprint diameter. The depth of the removed material $h = \beta\tau$ is proportional to the dwell time τ, defined by $\tau = YD/V$, with a proportionality constant $\beta = D_V/SD$. When $Y = 1$, which is the continuous mode, tool removal (dwell time) h is controlled by CNC velocity. When $Y < 1$, which is the pulsed mode, h is controlled by means of switching the slurry supply and keeping the tool velocity constant. The continuous mode is limited to removals greater than $h_{\{min\}} = D_V\, Y/V_{\{max\}}S$. In order to obtain a lower removal, the pulsed mode must be employed.

For a tool footprint diameter of 7 mm and a maximum CNC velocity of 2000 mm/min, the minimum period of the switching signal will be 0.2 seg, or 5 HZ, which is within the 10 Hz switching frequency range. In an extreme case, where the duty cycle is switched between 0 and 1 while maintaining a constant velocity, it is possible to create a pixelated pattern that is useful for determining the response function of the pulsed tool (**Figure 6b**). A fringed pattern can be observed where the interface between the regions presents a slope that corresponds to the tool footprint diameter, which is the limiting polishing element size (*poxel*, or polishing element).

3.2.2. Zonal polishing

When only a small section of the surface needs to be polished, this region must be approached with the tool turned on, leaving behind unwanted tracks, as well as approach and exit marks. This is solved by using the pulsed mode of the HyDRa tool. When an isolated region that needs further polishing is identified, a dampening band of constant width surrounding it is defined. Assuming a raster pattern is used, the region is approached with the HyDRa tool fully operational with $Y = 0$, until it enters the dampening region. Here velocity is smoothly incremented to the value needed inside the region while at the same time, the desired dwell time is controlled by means of PWM. The width of the dampening region is determined by the CNC acceleration and deceleration capabilities. Inside the region to be corrected, either a pulsed or continuous polishing can be used in order to maximize efficiency.

3.2.3. Pixel polishing

In the constant velocity PWM polishing case, the resulting response function in the sweep direction is different from the response function of the transverse, raster direction. When a symmetrical finishing is needed, it is possible to employ the pixel polishing method, which consists of stepping the tool at discrete positions with respect to each other, covering the region of interest with the same step increments in both axes. The tool is then switched on for the necessary time in order to achieve the desired removal for each position. This method can also be useful when very localized zonal polishing is needed. This allows the tool to either follow a raster pattern, or any other trajectory or set of discrete positions over the region of interest. An example of this method was used in Section 3.1 for the linearity test, where it was shown that a removal resolution of 0.1 nm can be attained.

3.2.4. Tessellated polishing

In the polishing of meter-class surfaces, efficiency is limited due to HyDRa's small footprint size and volumetric removal rate. Efficiency, however, can be improved by simultaneously polishing the surface with several HyDRa tools. These tools can be mounted on independent polishing robots, where each robot tackles a certain section of the surface. Alternatively, several tools can be mounted on a single robot arm, as described below. This method poses several problems, such as obtaining smooth seams between sections, approaching each section without leaving marks, and avoiding collisions as two tools concurrently approach the boundary between sections. In order to obtain a seamless interface between two independent sections, it is necessary to approach the boundary following special trajectories, such as the wedge pattern shown in **Figure 7** (bottom). This trajectory avoids duplicating dwell time at the seam, such as would happen if a rectangular pattern were used (top of **Figure 7**).

3.2.5. Polishing run interrupt

When the polishing process needs to be interrupted, it is now possible to stop at any point on the surface and continue polishing at a later time.

3.2.6. Edge problem

As in other polishing methods, the HyDRa tool tends to leave a small (one footprint diameter) fallen edge. In order to overcome this with the unmodified HyDRa tool, tool velocity is

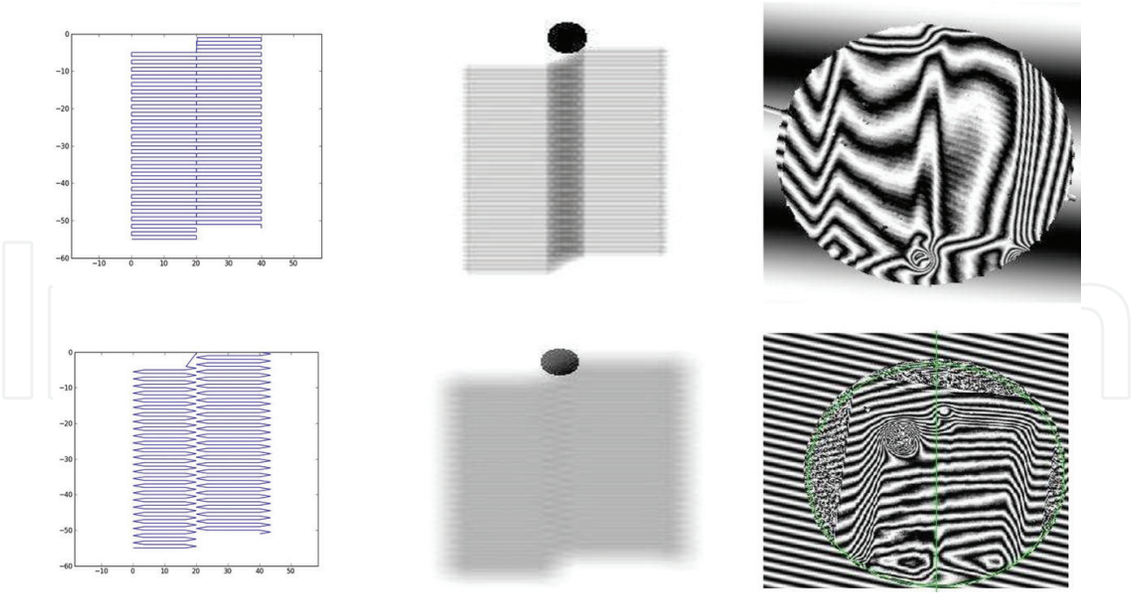

Figure 7. Tessellated polishing showing two different trajectory approaches. The figures to the left show the region of the interface between two raster patterns that use a rectangular (upper) and wedge (lower) seam at the boundary. The middle figures show a simulation of the resulting removal with the tool moving at a constant velocity and without PWM. Note the approach/exit tool mark at the beginning/end of the trajectory due to not switching the tool off. The interferograms to the right are actual polishing experiments. As can be seen, the raster pattern using rectangular trajectories duplicates removal at the seam, whereas the wedge trajectory produces a seamless interface. Another possible solution is to vary the pulse width at the seam, in order to match the dwell time between adjacent polishing sections.

http://dx.doi.org/10.5772/intechopen.75524

incremented as the tool approaches the edge, reducing dwell-time. This is counterintuitive and can present CNC control problems, since the tool is accelerated in a region where it should be preparing for a raster direction change. The on–off capability of the new tool can alleviate this problem, since dwell-time can be controlled without having to increment tool velocity at the edge region. In fact, this method allows for decelerating the CNC in order to prepare for a direction change.

3.2.7. Convergence

Another advantage of being able to pulse the tool is a quicker convergence towards the desired surface [10]. As pointed out in [11], the existence of a minimum amount that will be removed due to not being able to turn the tool off (h_{min}), limits the amount of material that can be removed in each run, whereas, by being able to pulse the tool, h_{min} can be made zero, allowing for a maximum value of f, further increasing the polishing convergence rate.

3.3. Multiple-head polishing

Since HyDRa tools can now be pulsed, several polishing heads can be mounted onto a common arm which moves at a constant velocity over the surface. Dwell time is then controlled using PWM for each tool, as required by the error map. We can also take advantage of the self-conforming capabilities of HyDRa, in that it is not necessary to employ a positioning device to conform the parallelism of the tool to the surface. Only one degree of freedom (DOF) per tool is required. Each loop is closed with a load cell signal and implemented by means of a linear stage, which permits zero-force polishing while freely following the local sag and tilt of the surface. Another advantage of this type of polishing is that one single slurry supply system can be used for all the tools, simplifying the system and considerably reducing the costs. Polishing efficiency becomes a function of the number of tools, and in the case of a matrix configuration, several polishing runs can be implemented into a single sweep, reducing polishing time.

By polishing with several tools, each tool is essentially given a section of the surface and the boundaries between sections are finished seamlessly, either by employing wedged joints, or by using PWM. Among the possible multi-tool configurations are matrix, linear and spiral layouts:

3.3.1. Linear

By mounting several HyDRa tools onto a single polishing arm, attached to a Cartesian CNC machine, it is possible to cover an area by sweeping the arm in the x and y directions. Each tool is separated from the next by a fixed distance δ in the x axis. The sweeping action in the x axis is done by moving the arm by δ, and then advancing with the selected raster step in the y axis. The overlap between the sections assigned to each tool is managed by either using tessellated or the PWM techniques, as described above. There are certain considerations to be taken into account for this method, particularly due to the edge problem that arises when polishing circular or non-rectangular surfaces. There will always be a tool that needs to either enter or exit the surface, while others are already polishing. Additionally, since these tools need to take advantage of their self-conforming capability, as they approach the edge of the workpiece, they loose floatability. These problems can be dealt with by adequate trajectory programming.

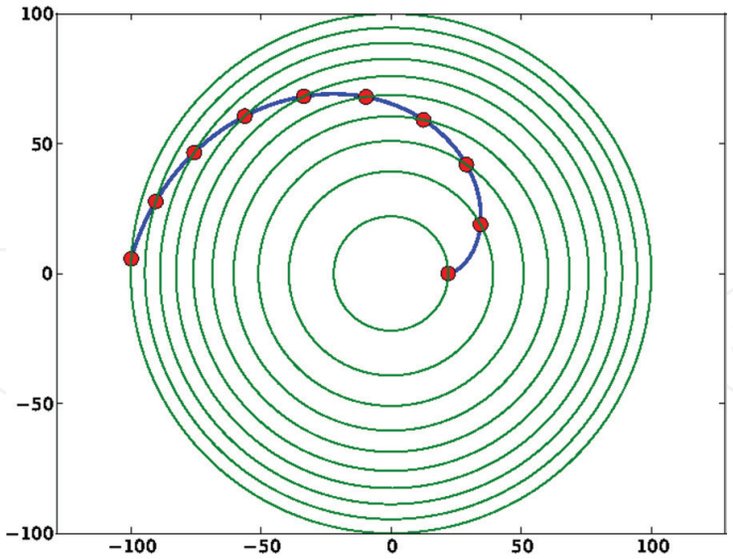

Figure 8. Hydra tools mounted on a spiral arm (see text).

3.3.2. Matrix

The linear configuration can be expanded by creating a matrix of tightly packed HyDRa tools maximizing tool number in order to minimize polishing time. The working principle is the same as the linear case, but adding *M* rows. This is equivalent to carrying out M polishing runs in a single iteration.

3.3.3. Spiral

In the case of large circular mirrors, it may be more efficient to polish the mirror by placing it on a rotary table. If we seek to fix as many HyDRa tools as possible onto a single arm, two conditions must be met. First, the number of tools should increase as r^2, so that each tool covers the same mirror area. Secondly, tools must be packed at the maximum allowable density, so that each tool sits next to the following one. Therefore, the shape of the arm must be a kind of spiral which is possible to solve for. By calculus of variations a spiral curve parameterized by the (increasing) radial coordinate, given in polar coordinates (r, θ) results in: $\theta(r) = \sqrt{4k^2 - 1/r^2} - \arctan\left(\sqrt{4(kr)^2 - 1}\right), r > 1/2k$. An example of this is shown in **Figure 8**, where HyDRa tools are mounted at equal separations along a spiral arm and may move along it to span equal areas, as the surface under it rotates.

4. Polishing parameters

Of the multiple finishing techniques currently in use, the ones based on sub-aperture polishing may be candidates for deterministic polishing, provided that the uncertainty of key polishing parameters is minimized. Deterministic polishing relies on a stable and predictable tool influence function; thus it is imperative that it is fully characterized for each material that will be

http://dx.doi.org/10.5772/intechopen.75524

polished. Simultaneously, metrology is a determining factor of the final quality of the surface, since it limits the precision of the error maps that can be obtained. This requires the knowledge of a series of polishing parameters such as tool velocity, pressure and height as well as slurry type, temperature, etc. Most of these parameters remain constant during the time periods required for polishing small optics, i.e. a few minutes. If larger, meter-class surfaces need to be polished, it is important to control and keep all parameters constant during an entire polishing run, which can represent over 10 h. Thus, a very stable and precise process control of the process is required.

The HyDRa tool removal function is based mainly on four independent operating parameters: propelling air pressure, grit mass concentration, height of the tool over the surface to be polished, and slurry flow and/or slurry pressure. In order to ensure deterministically polished surfaces, the errors contributed by each of these factors must be taken into account and precisely controlled to 1% for the entire length of the polishing run (over 100 h). Simultaneously, metrology is crucial for determining the surface's final quality, since it dictates the limit of the precision of the error maps that can be obtained.

4.1. Deterministic polishing

To maximize polishing performance, an abrasive foam is created in the tool's first stage. This raises the velocity of the polishing particles, improving the removal of material. This foam is produced by combining a constant flow f (a few ml/s) slurry, with air that is kept at a constant pressure P_p. This fluid is then accelerated with pressurized air at a propelling pressure P_T, in one or more cylindrical cavities. The resulting abrasive foam is then expelled through the tool's nozzle, where a vortex is produced that develops into a radial flow, and generates a grazing, uniform removal footprint. A relation of slurry flow f to slurry pressure P_p exists for each value of accelerating pressure P_T. This, in addition, depends on the tool's physical characteristics, such as its overall dimensions, the geometry of the acceleration chamber(s), as well as the nozzle shape. This relation establishes an operational diagram that defines tool bias. In this section, the control of f is chosen, although it is possible to select to control for either f or P_p. The removal D of HyDRa mainly depends on four independent operating parameters: propelling air pressure P_T, grit mass concentration ρ_i, slurry flow f, and distance of the tool over the workpiece Z. In order for deterministically polished surfaces to be obtained, the errors contributed by each of these parameters must be taken into account and controlled.

The removal rates, as determined by a series of independent experiments, where the polishing parameters varied, are shown in **Figure 9**.

To generalize the analysis, all parameters X are normalized around their operational values as x/x^-. With this, the relative variation of each parameter, defined as $\delta X = \frac{\Delta X}{X^-} = \Delta\left(\frac{X}{X^-}\right)$, is computed. The ratio between the relative variations of removal rate and the relative variations of each polishing parameter is given in the upper-left corner of the graphs. Here the operational value for the relative density is 80 g/l. As can be seen, removal rate varies as 1.18 times the fluctuations in the concentration. The relationship between the removal rate and the rest of the parameters can be determined similarly, where the fluctuations around the operation point of each parameter are taken into account. The sensitivities on

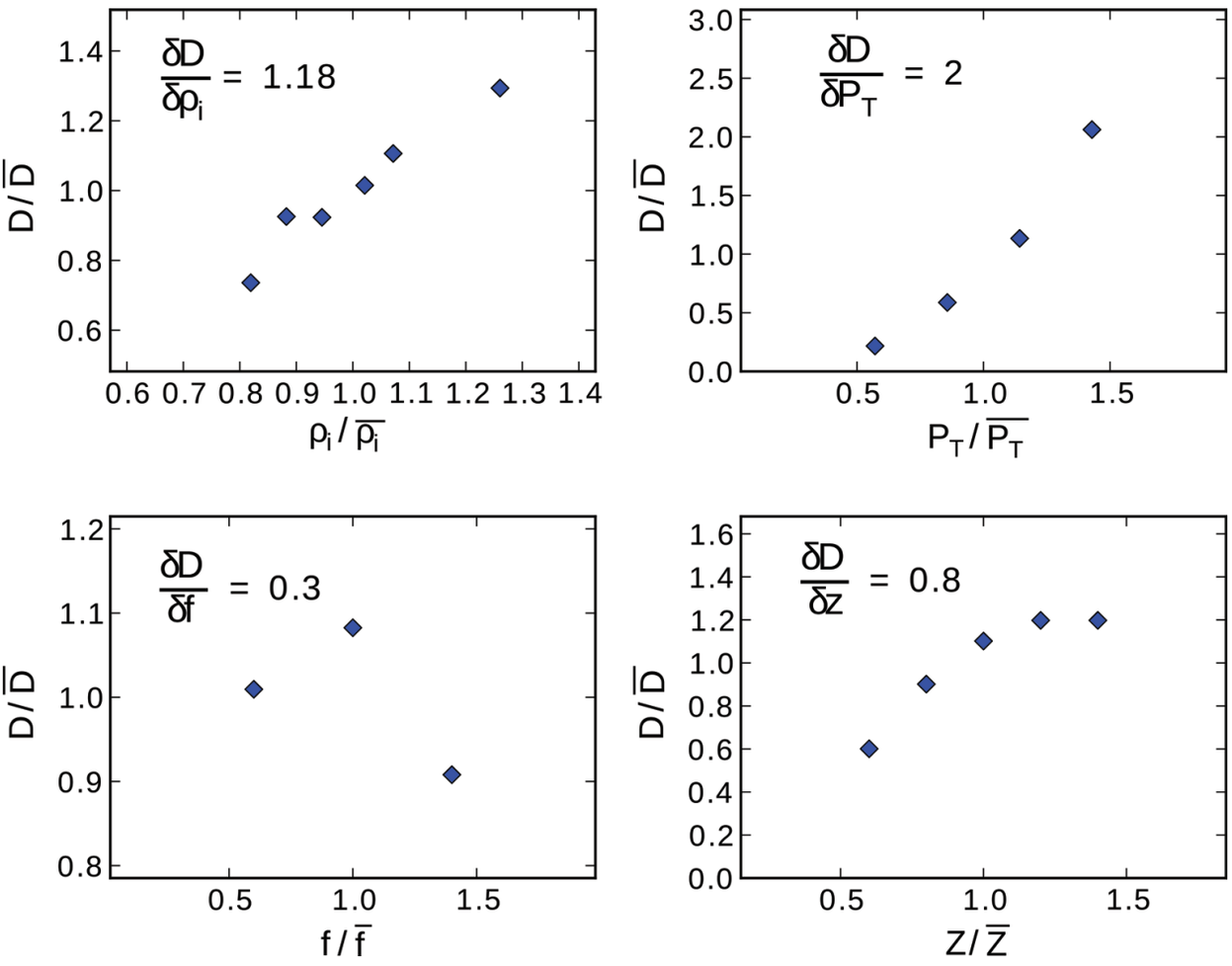

Figure 9. Normalized removal rate $D/\bar{D}$ (dimensionless) with reference to the normalized value of certain polishing parameters (mass concentration ϱ_i, propelling pressure P_T, slurry flow f and tool height z). The sensitivity of removal to each parameter is indicated in the upper left corner of each graph.

propelling pressure P_T (upper-right), slurry flow f (lower-left) and tool height z (lower-right) are 2, 0.3 and 0.8, respectively. In this test, the operation points were 40 PSI, 5 ml/s and 400 μm, respectively. An optimum value of slurry flow (around 5 ml/s), for which the removal rate is maximized and which is chosen to operate the HyDRa tools, can be found. Removal only decreases slightly for higher or lower flow rates around this value. This is shown in the lower left panel of **Figure 9**.

In the case of tool height z, load cell force F_c can be used instead, since, as shown in [4] tool force is an approximate linear function of distance when close to the operation point, given that $z + K F_c$, with $K \sim 10$ μm/N, and hence $\delta z = \delta F_c$.

If we assume that each of these four variables is statistically independent, the total error can be added in quadrature. For example, if each parameter is controlled to ~1% precision, then the total error δD_T is $\delta D_T = \sqrt{(1.18 * \delta\rho)^2 + (2 * \delta P_T)^2 + (0.3 * \delta f)^2 + (0.8 * \delta z)^2}$, which amounts to 2.5% for this case. This means that if 500 nm of material are removed in one polishing run, considering that the parameters are controlled to 1%, the total surface error results in 12.5 nm RMS (λ/50). This constitutes a 2.5% level of nondeterminism (i.e., 97.5% determinism).

http://dx.doi.org/10.5772/intechopen.75524

4.2. Polishing example: polishing of an 84 cm mirror

As mentioned before, in order to deterministically polish large surfaces it is imperative that removal rate remains stable over extended time periods. We polished an 84-cm hyperbolic primary mirror to $\lambda/10$ RMS, 0.7 λ PV in order to prove that HyDRa could deterministically tackle meter-class optics. The polishing process is described in [12]. From the error maps that were acquired during the iterations, the level of determinism of the process could be calculated. From each map we computed a tool trajectory with distinct dwell times. The amount of removed material was calculated by subtracting the previous error map from the measured one. Then, from the obtained result after polishing, the removed material for each iteration was determined and plotted as a function of dwell time. Refer to **Figure 10**. A linear relation is expected and the deviation from this represents the level of determinism, **Figure 11**. This experiment was useful to evaluate the importance of the stability of each parameter in the level of determinism for prolonged time periods. In the figure, a larger error can be noticed for shorter dwell-times than for longer ones. This is due to CNC errors when the tool has to be quickly accelerated to obtain short dwell-times. As the mirror is progressively corrected, the surface is smoother and these changes tend to decrease.

4.3. Polishing example: PSD and polishing of Fabry-Perot etalons

Three components in the power spectral density (PSD) of the residual surface errors that are related to the footprint diameter of the tool D_H exist for any given polishing method. In the low frequency domain ($L >> D_H$), the surface errors (optical figure) are a function of the stability of the polishing parameters during the polishing run, while at the high-frequency domain ($L << D_H$), the physics of the polishing process determine surface quality (micro-roughness). In the case of mid-spatial frequencies ($L \sim D_H$) surface quality depends on the geometry and overlap of the polishing trajectories. We obtained PSD measurements as described in [4] and references therein.

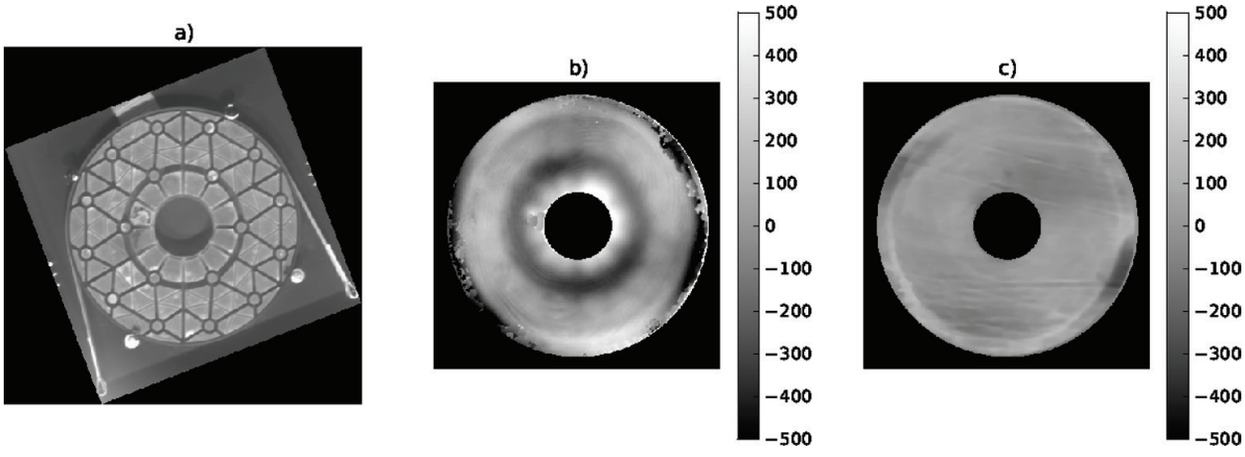

Figure 10. An 84 cm mirror with a 1 cm thick faceplate that was polished using the HyDRa system. (a) Picture of the mirror's internal back-structure. (b) Mirror prior to HyDRa finishing. The print-through left by the original lap-polishing process can be noted. (c) Mirror surface after HyDRa polishing. The polishing process entirely removed the print-through by polishing with the zero-force, error-map based process described in this chapter. Low-order Zernikes have been removed so this effect is highlighted. Z-scales are the same and are shown as vertical bars in nm.

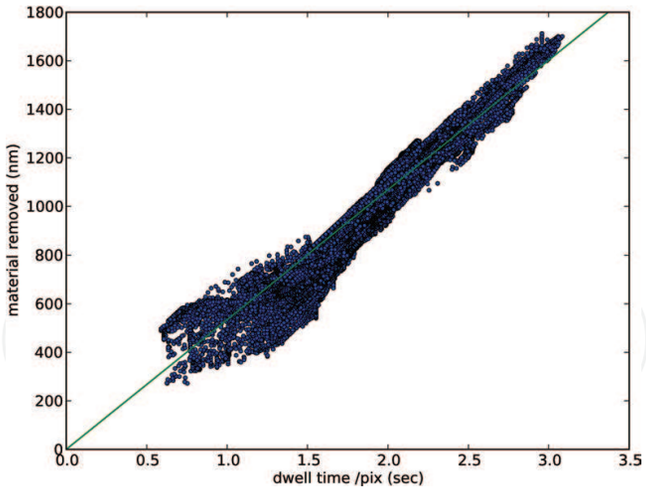

Figure 11. Total amount of material removed in the final iteration (3 runs = 30 h), as a function of dwell time in each area element of 2.6 × 2.6 mm^2 (pixel size). A linear relation at a removal rate of 13 mm^3/h (shown as a solid line) is expected for an entirely deterministic process. The true deviations from this behavior amount to 10.6%, which is the attained level of non-determinism and represents the standard deviation of the points with respect to the best-fit line.

The PSD is discussed using the results obtained while polishing four 50 mm etalon plates to better than $\lambda/100$. These 50 mm diameter water-free fused silica plates are used in an NIR scanning Fabry-Perot interferometer. These surfaces were polished using the HyDRa tool discussed in Section 4. Surface measurements were taken with a phase-shifting (PS) Fizeau interferometer in order to quantify the figure with a 180 μm pixel size projected onto the surface. A PS Linnik interferometer with 2× and 50× objectives (equivalent pixel sizes of 7.6 and 0.16 μm) was used to determine mid- and high-spatial frequencies, respectively. In **Figure 11a**, the 2-dimensional power spectrum PSD_2 vs. spatial frequency is plotted. It can be noted that three overlapping regimes exist that correspond to the series of instruments that were used to evaluate the surface quality. The integrated RMS values for each regime are 3.8, 1.5 and 2.9 nm for low-, mid- and high-spatial frequencies, respectively. The overall slope is approximately described as $f^{-2.5}$. Since in this section the physics of the HyDRa tool are described, emphasis will be made on the PSD high spatial-frequencies (micro-roughness). For lower frequencies, i.e. meter-class optics, where it is crucial to achieve a very high stability of the operational parameters, refer to [13]. **Figure 12b** shows one of four etalon plates that were polished.

Interferograms [10] showed initial figure errors that ranged between 27 and 83 nm. Using these measurements, we calculated the error maps to compute a dwell-time based raster pattern trajectory for the CNC polishing machine. An acceleration pressure of 40 PSI was chosen and tool height was controlled to achieve zero-force on the workpiece. RMS surface qualities between 3.6 and 6.8 nm were obtained after two 15 min polishing runs. The low frequency interval of the PSD shows an overall RMS fit to the desired figure of 3.8 nm, which is in accordance with the results presented in the previous section: a final surface figure quality of $>>\lambda/100$ for visible wavelengths. Sub-aperture polishing can introduce unwanted patterns associated with the polishing trajectories [14] which can occur in HyDRa polishing with a 7 mm footprint on a 40 mm sample. To minimize these mid-spatial frequencies, the tool was raster-scanned with 0.25 mm steps, which corresponds to 1/20th of the tool's footprint size.

http://dx.doi.org/10.5772/intechopen.75524

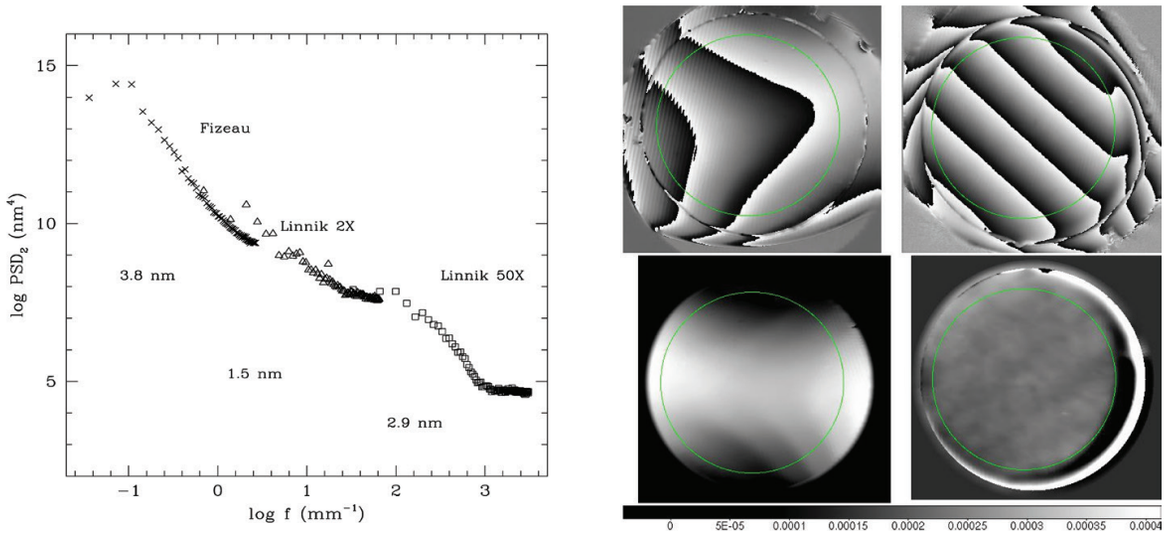

Figure 12. (a) 2-D power spectral density PSD_2 as a function of linear spatial frequency obtained with HyDRa on an etalon plate. (b) One of four etalon plates prior and after HyDRa polishing. The wrapped phase of the surface before (left) and after (right) polishing is shown in the upper images. Unwrapped phases of the original and polished surface, respectively (lower images). The inscribed green circle delimits the plate's usable region. Of the 50 mm plate diameter, only the central 40 mm were polished, since the exterior ring is used for mounting the plates. This area is indicated within the light-colored circle.

Traces of this raster pattern should have been visible in the 0.14–4 mm^{-1} frequency range on the PSD. However, no evident peaks that could have been related to grooves left by a raster pattern could be observed, and only a tiny peak corresponding to about 100 μm could be noted. This peak adds a very small fraction of a nm to the total 1.5 nm RMS of the mid-frequency band, demonstrating that "over-rastering" can be effective in minimizing mid-spatial frequencies. This represents an alternative to the approach proposed by Fähnle [15], using only one tool. A comparatively large footprint has the extra advantage of making our process insensitive to CNC positioning errors, which are two orders of magnitude smaller than the footprint size. Finally, the high-spatial frequency domain shows an RMS of close to 3 nm. Although the PSD decreases in this region, it apparently stabilizes at frequencies $>10^3$ mm^{-1} or sizes smaller than 1 μm. This number is related to the grit size that was used in this test. To sustain a decreasing PSD tendency and thus, smaller values of the high-frequency RMS, the use of smaller grit sizes is suggested. Integrating the high-frequency domain of the PSD to obtain the RMS is also equivalent to calculating the RMS directly from a 50 × 50 μm area of the micro-interferogram, according to a standard definition of micro-roughness [16]. This micro-roughness obtained with the HyDRa process (3 nm) is comparable to the roughness reported in current FJP literature [5].

Acknowledgements

This work was funded by Universidad Nacional Autónoma de México DGAPA-PAPIIT grants IN112505, IN115509, IT100216 and IT100118, as well as by Instituto de Astronomía, UNAM.

Author details

Erika Sohn*, Esteban Luna, Elfego Ruiz, Luis Salas and Joel Herrera

*Address all correspondence to: sohn@astro.unam.mx

National Autonomous University of Mexico (Universidad Nacional Autónoma de México), Institute for Astronomy, Ensenada, BC, México

References

[1] Ruiz E, Sohn E, Salas L, Luna E. Hydrodynamic radial flux tool for polishing and grinding optical and semiconductor surfaces. 2007. US Patent 7169012

[2] Ruiz E, Sohn E, Salas L, Luna E. Modulo mezclador para una herramienta hidrodinamica deterministica para el pulido pulsado de superficies opticas, y metodo para llevar a cabo el pulido pulsado. PCT Patent Application. UNAM.REG.OMPIPCT/MX/a/2016/016317

[3] Li Z, Li S, Dai Y, Peng X. Optimization and application of influence function in abrasive jet polishing. Applied Optics. 2010;**49**:2947-2953

[4] Sohn E, Ruiz E, Salas L, Luna E, Herrera J. HyDRa: Polishing with a vortex. Applied Optics. 2013;**52**:6146-6152

[5] Fähnle OW, van Brug H, Frankena H. Fluid jet polishing of optical surfaces. Applied Optics. 1998;**37**:6771-6773

[6] Shi C, Yuan J, Wu F, Wan Y. Ultra-precision figuring using submerged jet polishing. 2011. COL 092201

[7] Arnold T, Böhm G, Fechner R, Meister J, Nickel A, Frost F, Hänsel T, Schindler A. Ultra-precision surface finishing by ion beam and plasma jet techniques-status and outlook. Nuclear Instruments and Methods in Physics Research A. 2010;**616**:147-156

[8] Guo P, Fang H, Yu J. Edge effect in fluid jet polishing. Applied Optics. 2006;**45**:6729-6735

[9] Joel HV, Esteban Antolin LA, Fernando QP, Elfego Guillermo RS, Luis SC, Erika SL. Programa de Computo de Evaluacion de Error Ygeneracionde Trayectorias HYTPT. Software Copyright, Universidad Nacional Autonoma de Mexico, 03-2012-120612154800-01. Mexico: INDAUTOR; 2012

[10] Luna E, Salas L, Sohn E, Ruiz E, Nunez JM, Herrera J. Deterministic convergence in iterative phase shifting. Applied Optics. 2009;**48**:1494-1501

[11] Salas L, Luna E, Sohn E, Ruiz E, Herrera J. HyDRa: Polishing process convergence rate optimization. Applied Optics. 2013;**52**:7007-7010

[12] Sohn E, Ruiz E, Salas L, Luna E, Herrera J, Quiros F, Nunez M, Lopez E. Polishing results of an 84 cm primary mirror with HyDRa. In: Proceedings of the SPIE Optifab, TD07-17; 2011

[13] Ruiz E, Salas L, Sohn E, Luna E, Herrera J, Quiros F. HyDRa: Control of parameters for deterministic polishing. Optics Express. 2013;**21**:20334-20345

[14] Dunn CR, Walker DD. Pseudo-random tool paths for CNC sub-aperture polishing and other applications. Optics Express. 2008;**16**:18942-18949

[15] Fähnle O, Mourad S, Hauser K, Meeder M. Detection and removal of spatial mid-frequencies in sub-aperture finishing. In: OSA IODC OFT, OWE4; 2010

[16] Nunez M, Salinas J, Luna E, Salas L, Ruiz E, Sohn E, Nava A, Cruz-Gonzalez I, Martinez B. Surface roughness results using a hydrodynamic polishing tool (HyDra). SPIE. 2004;**5494**: 459-467

IntechOpen